Liquid Crystals
Publication details, including instructions for authors and subscription information:
http://www.informaworld.com/smpp/title~content=t713926090

Orientational ordering in some nematogens deviating from the classical rod-shape

Felix Perez; Patrick Judeinstein; Jean-Pierre Bayle; Hassan Allouchi; Michel Cotrait; Frederick Roussel; Bing M. Fung

Online publication date: 06 August 2010

To cite this Article Perez, Felix , Judeinstein, Patrick , Bayle, Jean-Pierre , Allouchi, Hassan , Cotrait, Michel , Roussel, Frederick and Fung, Bing M.(1998) 'Orientational ordering in some nematogens deviating from the classical rod-shape', Liquid Crystals, 24: 4, 627 — 637
To link to this Article: DOI: 10.1080/026782998207118
URL: http://dx.doi.org/10.1080/026782998207118

LIQUID CRYSTALS, 1998, VOL. 24, NO. 4, 627–637

Orientational ordering in some nematogens deviating from the classical rod-shape

by FÉLIX PEREZ, PATRICK JUDEINSTEIN, JEAN-PIERRE BAYLE*
Laboratoire de Chimie Structurale Organique, Université Paris XI. U.R.A. 1384, 91405 Orsay Cedex, France

HASSAN ALLOUCHI, MICHEL COTRAIT
Laboratoire de Cristallographie et de Physique Cristalline, E.R.S.133 CNRS, 351 Cours de la Libération, Université Bordeaux I, 33405 Talence Cedex, France

FRÉDÉRICK ROUSSEL† and BING M. FUNG
Department of Chemistry and Biochemistry, University of Oklahoma, Norman, Oklahoma 73019-0370, USA

(*Received 8 September 1997; accepted 12 November 1997*)

Several new laterally substituted liquid crystalline compounds have been synthesized. They have the same main core which contains four rings (two aromatic, two alicyclic) with two lateral substituents introduced on the same side of one of the inner rings. One of the substituents is a 4-*X*-benzyloxy group ($X = CH_3$, CN, Cl) and the other is a hexyloxy chain. The presence of the lateral aromatic substituent makes these compounds deviate markedly from the classical rod-shape. However, a wide enantiotropic nematic phase is present for all the compounds. The order parameters of the chain and the *para*-disubstituted aromatic rings were obtained by using a 2D ^{13}C NMR technique with variable angle spinning. The temperature dependence of the order parameters was estimated using ^{13}C chemical shifts with slow spinning of the sample parallel to the magnetic field. The results indicate that the two lateral substituents are more or less folded back along the mesogenic core. Thus, the flexible lateral chain is found to be roughly aligned with the molecular long axis, whereas the *para*-axis of the less flexible aromatic branch makes a considerable angle with the molecular long axis imposed by the core, substantially increasing the mean width of the molecule. The core ordering does not seem to be influenced by the type and position of the substituents. The folding back of the lateral chain and the substantial tilt of the lateral aromatic branch with respect to the core main axis are confirmed by the X-ray structure of a parent compound.

1. Introduction

Although large lateral substituents generally reduce the mesogenic property of rod-like compounds, they do not always destroy the liquid crystal arrangement [1]. Depending on the flexibility of the lateral fragments attached to the core, two different situations can be encountered.

If the flexibility of the lateral fragment is rather high, as for an alkyl or alkoxy chain, the liquid crystalline arrangement can be preserved due to the special conformation adopted by the chain in the mesophase [2–6]. Our previous NMR studies have revealed that when an alkoxy chain is introduced into the centre part of the core, it is folded back along the molecular long axis due to the anisotropic forces encountered in the nematic phase [7–9]. The orderings of the methylene groups are quite constant along the chain, indicating a nearly uniform conformational disordering of the entire lateral chain. Lateral chains are certainly less free to move than terminal chains. If the flexibility of the first fragment is not sufficient to permit the alignment of the substituent along the core, the major axis of the substituent can form a non-negligible angle with the core, substantially increasing the width of the molecule. As a consequence, the mesogenic core needs to be sufficiently long in order to preserve the liquid crystal properties [1].

When the lateral substituent contains a ring with a short spacer, the flexibility decreases substantially. In a previous paper, we reported two homologous series of

* Author for correspondence.
† On leave from Laboratoire de Dynamique et Structure des Matériaux Moléculaires, Université du Littoral, U.R.A. 801, MREID, 59140 Dunkerque, France.

0267–8292/98 $12·00

compounds containing four aromatic rings in the main core and two lateral substituents on one of the inner rings, one alkoxy chain and a 4-chlorobenzyloxy branch; they exhibited the nematic phase [1]. The nematic range was found to be slightly dependent on the relative position of the lateral aromatic branch. By applying a 2D NMR technique, the orientational ordering of the aliphatic part of two isomeric compounds was obtained. The two lateral chains were found to be folded back along the mesogenic core, involving a *gauche*-conformation for the first segment. The molecular long axis of the core seemed not to be influenced by the pattern of disubstitution. By molecular modelling, it was found that the *para*-axis of the lateral aromatic ring makes a non-negligible angle with respect to the core [1].

In the present paper, in order to obtain a better view of the aromatic ordering, we present the synthesis of some related compounds containing fewer aromatic rings in the main core. These compounds contain a core with a different four-ring system (two aromatic, two alicyclic) with a hexyloxy lateral chain and a lateral aromatic ring. This lateral aromatic ring is *para*-substituted by a non-polar (–CH_3), a medium polar (–Cl), or a strongly polar group (–CN). The decrease in the number of aromatic rings in the compounds results in less complex ^{13}C NMR spectra, and enables us to assign the peaks for the study of the ordering of the two *para*-disubstituted phenyl rings by 1D and 2D NMR. Then, the effect of the terminal group borne by the lateral aromatic branch on the mesomorphic properties is discussed. In addition, the X-ray structure of a parent compound having an identical inner core is presented.

2. Experimental

2.1. *Synthesis*

The two series: 2-(4-*X*-benzyloxy)-3-*n*-hexyloxy-4-(*trans*-4-*n*-pentylcyclohexanoyloxy)-4′-(4-*n*-pentylcyclohexanoyloxy)azobenzenes (**6R*X***) and 3-(4-*X*-benzyloxy)-2-*n*-hexyloxy-4-(*trans*-4-*n*-pentylcyclohexanoyloxy)-4′-(4-*n*-pentylcyclohexanoyloxy)azobenzenes (**6L*X***) are depicted in figure 1 and were prepared according to identical procedures. *X* is CH_3, Cl or CN. As an example, the synthetic scheme for **6RCl** is presented in figure 2 and the synthesis is briefly described below.

2-(4-Chlorobenzyloxy)-3-*n*-hexyloxyphenol was prepared in two steps by selective etherification of 1,2,3-trihydroxybenzene (THB) using a procedure detailed elsewhere [10]. *p*-Toluic acid was esterified with 4-nitrophenol using the well-known DCC method [11]. Then, the selective reduction of the nitro group was achieved using the $NiCl_2/NaBH_4$ reducing system [12]. The crude solid substituted aniline hydrochloride was used for the diazotization step. Then, the coupling step

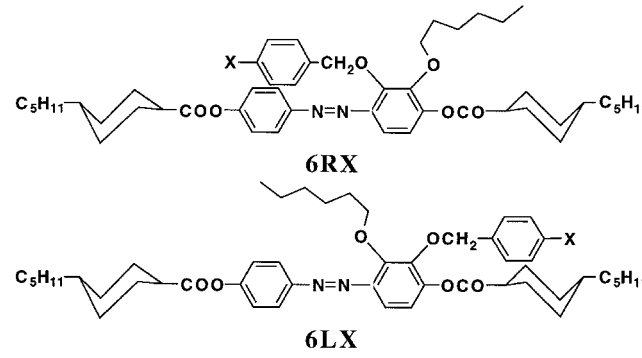

Figure 1. Molecular structures of the members of the two series synthesized.

was performed, using PEG 200 as solvent, between the diazonium salt and the dialkoxyphenol under basic conditions [1]. Coupling occurs mainly in the position *para*- to the remaining hydroxyl group. Four molar equivalents of NaOH were then added directly in the PEG mixture, and the flask was heated at 100°C for 2 h in order to saponify the ester bond. After cooling, some water was added and the pH was carefully adjusted to 5·5. The mixture was shaken with three portions of ether and the extracts were washed three times with water and then three times with acidified water. After drying and evaporating the solvent, the crude product was chromatographed on silica gel (60–200 mesh) with CH_2Cl_2/ethyl acetate (80/20) as eluent, and the diphenol was collected as the last fraction. Finally, the diphenol was esterified with the *trans*-4-*n*-pentylcyclohexane-1-carboxylic acid chloride in $CHCl_3$/pyridine as solvent. After chromatography (silica gel 60–200 mesh, eluent $CHCl_3$, first fraction), the final product was recrystallized from a mixture toluene/ethanol/4-methylpentan-2-one (10/80/10) until constant transition points were obtained. These transition points were measured by DSC (Mettler FP 52) using a heating rate of 10°C min^{-1}.

2.2. *X-ray data collection and structure resolution*

We were not able to obtain single crystals of compounds with two terminal 4-pentylcyclohexane carboxylate groups. However, suitable crystals of a related compound having five aromatic rings were easily obtained. Thus, single crystals of 2-(4-chlorobenzyloxy)-3-*n*-octyloxy-4-(4-chlorobenzoyloxy)-4′-(4-methylbenzoyloxy)-azobenzene compound were grown from $CHCl_3$ solution at 293 K. The cell parameters were obtained and data collection performed with a CAD-4 Enraf-Nonius diffractometer, equipped with a graphite monochromator. The crystal data, the data collection conditions and the refinement characteristics are given in table 1. The reduced crystal data were obtained using the SDP package [13]. The crystal structure was

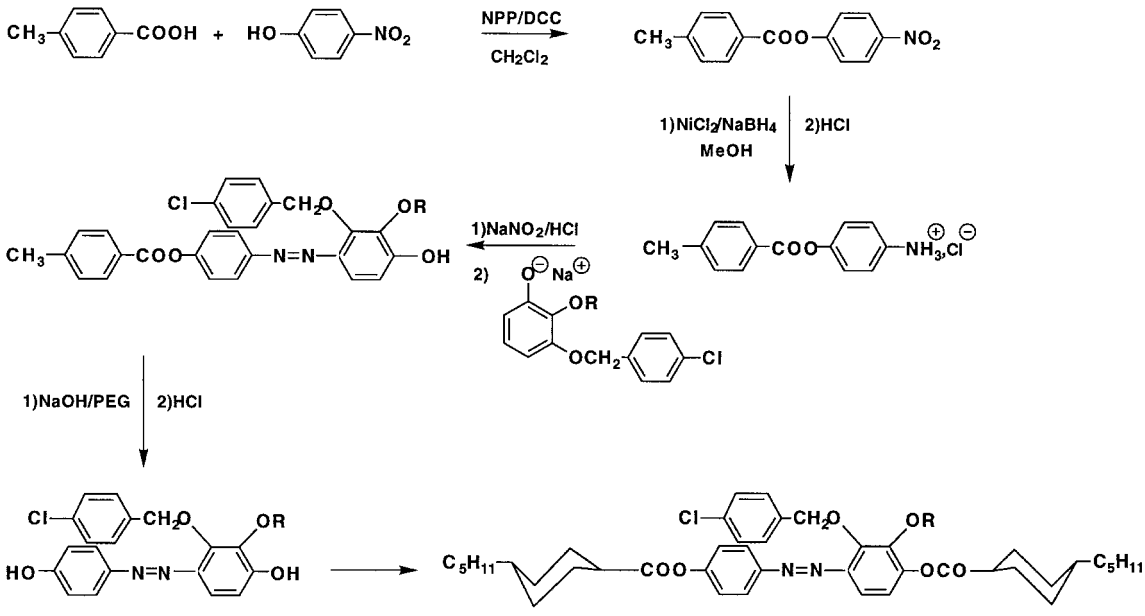

Figure 2. Synthetic scheme for 3-(4-chlorobenzyloxy)-2-*n*-hexyloxy-4-(*trans*-4-*n*-pentylcyclohexanoyloxy)-4′-(4-*n*-pentylcyclohexanoyloxy)azobenzene.

Table 1. Crystal data, data collection conditions and refinement characteristics.

Crystal data			
Chemical formula	$C_{42}H_{40}N_2O_6Cl_2$	MW/g mol^{-1}	739·7
Crystal system	triclinic	Space group	*P*1
a/Å	21·963(1)	*α*/°	89·273(8)
b/Å	11·308(1)	*β*/°	85·469(6)
c/Å	16·090(2)	*γ*/°	78·889(6)
Volume of cell/Å^3	3909	no. of molecules per unit cell (*Z*)	4
Density/g cm^{-3}	1·257	absorption *μ*/mm^{-1}	1·891
Crystal shape	prism	crystal colour	red
Data collection conditions			
Radiation	CuK_α	wavelength/Å	1·54178
Number of reflections for cell parameters and crystal setting	25	*θ* range/°	21–35
Temperature	293 K	scan	*ω*-2*θ*
h_{min}, h_{max}	−24, 24	θ_{max}/°	60
k_{min}, k_{max}	0, 12	standard reflections	3
l_{min}, l_{max}	−18, 18	absorption correction	none
measured reflections	11 593	observed reflections	5174
Refinement			
Refinement mode	on *F*	weight *w*	$1/\sigma(F)^2$
R	0·056	*wR*	0·064
Goodness of fit *S*	1·73	number of refined parameters	937

solved by direct methods, using the Shelx 86 package [14]. Two independent molecules were found in the asymmetric cell. The position of the atoms of the polyaromatic central cores and of the 4-chlorobenzyloxy lateral group of both independent molecules were obtained in the first calculation, as well as the first atoms of the octyloxy chains. The remaining atoms of the octyloxy lateral chains were located, with some difficulty, after successive difference Fourier synthesis.

Atomic parameters were refined isotropically, then anisotropically with a local program called Crisaf. Then, hydrogen atoms were introduced in their theoretical positions, with isotropic thermal motion factors B_i of the carbon to which they were attached and the

refinement was resumed. The atomic scattering factors were taken from the International Tables for X-ray Crystallography (1974, Vol. IV). The final reliability factors were $R = 0{\cdot}056$ and $wR = 0{\cdot}064$ with a goodness of fit $S = 1{\cdot}74$.

2.3. *NMR experiments*

The 2D ^{13}C NMR experiments using separated local field spectroscopy (SLF) with variable angle spinning (VAS) [15, 16] were performed using a Varian XL-300 NMR spectrometer at $B_o = 7{\cdot}05$ T. The angle between the spinning axis and the magnetic field was set at *c.* 45°. The exact value of the angle was determined for each experiment by measuring the ratio of the F–F dipolar coupling of 2,2,-difluoro-1,1,1,2-tetrachloroethane dissolved in the nematic phase of ZLI-1291 with and without sample spinning. The data from the XL-300 NMR spectrometer were processed on a VXR-4000 data station [16]. Three compounds were investigated **6RCl**, **6LCl** and **6RCH3**.

Slow spinning ^{13}C NMR experiments were performed on four compounds (**6RCl**, **6LCl**, **6RCH3** and **6LCH3**) using a Varian VXR-500 NMR spectrometer ($B_o = 11{\cdot}07$ T) equipped with an indirect detection probe manufactured by Narolac Cryogenic Corporation. The sample was put in a standard 5 mm tube and spun along the magnetic field so that the director aligned parallel to the magnetic field. To avoid rf overheating, a 0·8% decoupler duty cycle was used. The temperature calibration was made by observing the nematic to isotropic transition.

3. Results and discussion

3.1. *Transition temperatures*

The transition temperatures and the $\Delta S_{NI}/R$ values of the six compounds synthesized are given in table 2. An enantiotropic mesophase with a wide nematic range is obtained (figure 3). This nematic range is larger than for the homologous compounds containing four aromatic rings [1], which is a consequence of the replacement of the aromatic rings bearing terminal methyl and chlorine groups by the two cyclohexane rings substituted by a terminal pentyl chain. Amazingly, the clearing temperatures show very little dependence on the terminal group introduced on the lateral branch. Usually, when a rigid lateral substituent is introduced directly on the core, the anisotropic broadening of the molecule perturbs the cooperative packing needed to form the mesophase so that the change in the clearing temperature is related to its van der Waals radius [17]. In our series, the lack of influence of the terminal group on the transition temperatures is due to the simultaneous presence of a lateral chain, which also enlarges the cross section of the molecule and partially hides the broadening effect of the

Table 2. Transition temperatures (in °C) and related entropies (in parenthesis) for compounds in the **6L*X*** and **6R*X*** series. These values are taken with increasing temperature (heating rate 10°C min^{-1}).

X	Chain Position	Cr	→ ($\Delta S_{KN}/R$)	N	→ ($\Delta S_{NI}/R$)	I
CH_3	R	•	74 (35·2)	•	150·5 (0·8)	•
CH_3	L	•	55 (44·7)	•	162·5 (1·1)	•
Cl	R	•	62 (27·8)	•	143·5 (0·9)	•
Cl	L	•	66 (37·8)	•	163 (1·0)	•
CN	R	•	77 (47·6)	•	146·5 (0·5)	•
CN	L	•	96 (31·6)	•	159 (0·4)	•

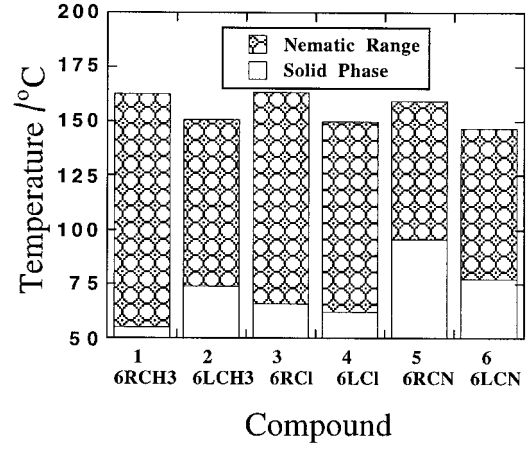

Figure 3. Nematic ranges for the two series. The transition points were measured by DSC (Mettler FP 52) using a heating rate of 10°C min^{-1}.

aromatic branch. It can be seen that this effect is less important for the **L** series. The melting temperatures are slightly higher for the compounds having the cyano group in the *para*-position of the lateral phenyl ring, which may result from some dipole–dipole interactions in the solid phase. Nevertheless, to increase the mesophase stability, the largest substituent has to point towards the centre of the molecule.

The values of $\Delta S_{NI}/R$ (table 2) have the same order of magnitude as for other published compounds with a lateral aromatic branch [1]. The actual values are in the same range as for the corresponding compounds containing a single lateral chain ($\Delta S_{NI}/R$ typically in the range of 0·5 to 0·8) [9] and larger than for those containing two alkoxy chains ($\Delta S_{NI}/R$ typically in the range of 0·15 to 0·2) [8]. This indicates that the lateral

aromatic branch does not add to the conformational entropy.

3.2. *Ordering of the lateral chains*

The dipolar splittings of the aliphatic parts of the **6LCl** and **6RCl** spectra in the nematic phase were obtained by using the 2-D VAS/SLF technique. The corresponding peaks of the two alicyclic rings essentially coincide with each other, and an analysis of the dipolar couplings was not made. The carbon assignment below 35 ppm was made according to previous studies [1] and can be verified in the 2-D experiment by the fact that a particularly complex shape is associated with carbons belonging to the cyclohexane ring and that the dipolar couplings of the terminal pentyl chain are larger than those for the lateral chain. In the OCH_2 region, we used the previous assignments obtained for the ***n*LC** and ***n*RC** series [1]. The downfield peak is assigned to the first chain carbon in the *ortho*-position with respect to the ester linkage, and the upfield peak to the chain carbon in the *ortho*-position with respect to the azo linkage. In the 2-D experiment, the OCH_2 group in the chain appears as a triplet for both compounds, whereas the OCH_2 group in the lateral aromatic branch appears as a singlet for **6LCl** and a small triplet for **6RCl**. All the other upfield aliphatic methylene carbons show the expected triplets in the $\omega 1$ dimension.

The splitting for the OCH_2 group belonging to the chains is smaller than those for the other methylene carbons within the lateral chain, which are, in turn, far smaller than those belonging to the terminal pentyl chain. The C–H bond order parameters S_{C-H} are generally negative for the CH_2 and CH_3 groups in the chain. They are related to the corresponding dipolar coupling constants (D_{C-H}) by:

$$S_{C-H} = -4{\cdot}407 \times 10^{-5} D_{C-H}. \qquad (1)$$

However, the S_{C-H} values for the lateral OCH_2 carbons are positive and the related dipolar coupling constants are negative [equation (1)] [8]. The dipolar coupling constants can be extracted from the observed carbon–proton splitting ($\Delta\nu$) in the 2-D experiment using equation (2):

$$\Delta\nu = f[(3\cos^2\beta - 1)D_{C-H} + J] \qquad (2)$$

where f is the scaling factor, which is equal to 0·420 for a BLEW-48 decoupling sequence, J is the scalar coupling constant determined from the coupled isotropic spectrum, and β is the angle between the spinning axis and the magnetic field.

Figure 4 shows the smooth decrease in the absolute values of the lateral chain order parameters for **6RCl** and **6LCl** in the same range of reduced temperature T/T_{NI}. The variation of the order parameter within the chain is relatively small, and the well-known odd–even effect of the order parameter values is not observed. The replacement of the terminal aromatic groups [1] by the two alicyclic groups does not change the ordering of the lateral chain grafted on the inner part of the core. As previously observed, the chains in the two isomers do not behave in exactly the same way [1]. In **6LCl**, the alkoxy chain points in the direction of the carboxylate link and overlaps with cyclohexyl ring which has high conformational disordering, whereas the chain in **6RCl** points in the direction of the azo link and overlaps a less disordered aromatic ring.

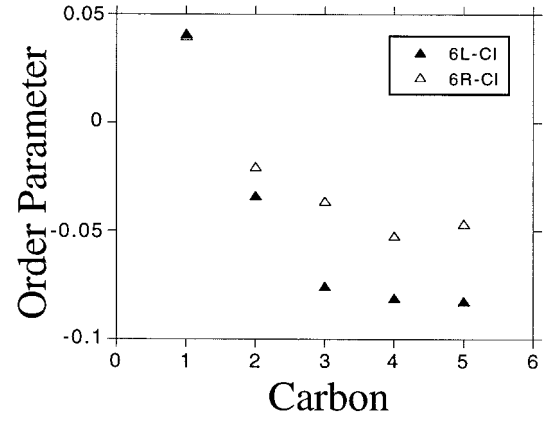

Figure 4. Comparison of the C–H bond order parameters for the lateral chains in the two isomeric compounds **6LCl** and **6RCl**.

3.3. *Ordering of the aromatic rings*

The aromatic part of the VAS ^{13}C spectra of **6LCl** in the nematic phase using the 2-D SLF technique is shown in figure 5. All 16 peaks are resolved, and the assignment was made according to the group contribution method to the type of pattern observed in the second dimension (given below the spectrum), and with respect to our previous studies on similar compounds [1, 8, 9]. The carbon–proton dipolar splittings of the protonated aromatic carbons and quaternary carbons belonging to the lateral aromatic branch are shown at the bottom of figure 5 for both compounds **6RCl** and **6LCl** (**6RCH3** is not presented, due to its very similar behaviour) at similar reduced temperatures. The traces for carbons C12, C13, C7 and C6 are quite different.

Before analysing these differences, let us consider the C–H coupling patterns expected for conventional nematogens. When the C_2 axis of a *para*-disubstituted aromatic ring is nearly aligned with the molecular long axis, a doublet of doublets is observed in the $\omega 1$ dimension for each protonated carbon belonging to that ring. This doublet of doublets occurs from the couplings between the carbon atom and the directly bonded hydrogen and the *ortho*-hydrogen, respectively. These coupling

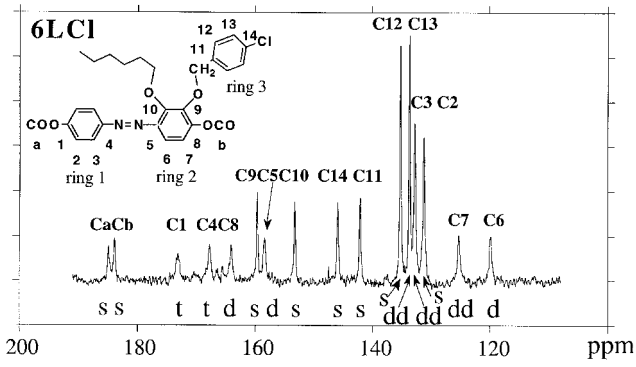

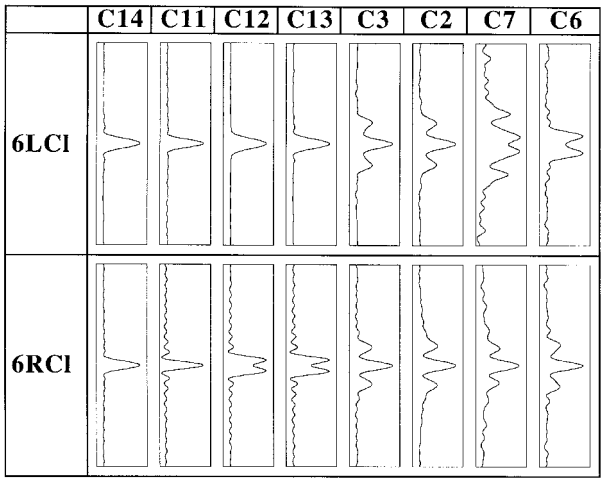

Figure 5. Aromatic part of the carbon ^{13}C VAS/SLF spectrum of **6LCl** at 75 MHz: temperature = 98·5°C; $\theta = 44{\cdot}8°$; spinning rate = 1·0 kHz. Dipolar traces for selected carbons are shown at the bottom of the figure for the two isomeric compounds **6RCl** and **6LCl**.

constants depend on the C–H distance and the angles between the C–H vector and the *para*-axis (defined as the z axis) as given by equation (3):

$$D_{C-H} = -\frac{\gamma_C \gamma_H h}{8\pi^3 r_{C-H}^3}[(3\cos^2\theta_{CH\text{-}z} - 1)S_{zz} + (\cos^2\theta_{CH\text{-}x} - \cos^2\theta_{CH\text{-}y})(S_{xx} - S_{yy})]. \quad (3)$$

The quaternary carbons display a nice small triplet due to the couplings with the two equivalent *ortho*-hydrogens. Indeed, for the aromatic ring in the core without substituents (ring 1), small triplets are observed for the quaternary carbons (not shown), and a doublet of doublets is observed for the protonated carbons C2 and C3 (figure 5). Because the factor $(3\cos^2\theta - 1)/r^3$ has similar values for the *ipso*- and *ortho*-C–H pairs and the second term in equation (3) is quite small, the corresponding values of D_{C-H} are not too different, and the splitting pattern looks like a triplet. On the other hand, the lateral phenyl ring (ring 3) shows really unusual patterns for the protonated (C12, C13) and quaternary (C11, C14) carbons. The reason for this will be discussed later.

The *para*-disubstituted aromatic rings undergo rapid jumps about their *para*-axes. Therefore, only two order parameters S_{zz} and $S_{xx} - S_{yy}$ are required to define the ring ordering. Because the dipolar coupling constant can be obtained from equation (2), the order parameters of ring 2 can be calculated by fitting the data into equation (3). The ring order parameter values in the three compounds studied are given in table 3, which shows that the values of S_{zz} are nearly equal in the same range of reduced temperature. This implies that the relative position of the lateral branch does not markedly influence the position of the molecular long axis. Because the whole molecule is no longer rod-like, the biaxiality of this ring is somewhat larger than for normal nematics, for which $S_{xx} - S_{yy}$ is typically 0·03.

For the compound **6LCl**, carbons C11, C12, C13 and C14 exhibit a single peak in the ω1 dimension (figure 5), indicating that the dipolar splittings are too small to be observed. This is a strong indication that the *para*-axis of the lateral aromatic ring makes an angle close to the magic angle (54·7°) with respect to the molecular long axis, so that the term $(3\cos^2\theta - 1)$ in equation (3) is nearly zero. For compounds **6RCl** or **6RCH3**, a small splitting reappears for carbons C12 and C13. Furthermore, for the ring with the lateral substituents (ring 2), the splitting patterns for carbons C6 and C7 show a tremendous difference for the two types of compound. As already noted for some laterally dimethylated compounds, every rigid part inside the mesogens

Table 3. Order parameters for the core phenyl ring *para*-disubstituted at different values of T/T_{NI} for **6RCl**, **6LCl** and **6RCH3**. The values were obtained from the dipolar couplings assuming fixed C–C–H angles within the aromatic rings. The absolute error is estimated at 5%.

Compound	T/T_{NI}	S_{zz}	$S_{xx} - S_{yy}$
6RCl	0·895	0·562	0·093
	0·871	0·581	0·095
	0·859	0·593	0·095
	0·847	0·606	0·098
	0·823	0·643	0·104
6LCl	0·854	0·613	0·114
	0·843	0·624	0·116
	0·831	0·626	0·115
	0·820	0·632	0·115
	0·809	0·639	0·118
	0·786	0·650	0·121
6RCH3	0·891	0·565	0·054
	0·880	0·578	0·054
	0·856	0·586	0·054
	0·844	0·597	0·058
	0·821	0·611	0·059

can orient in a particular way [19, 20]. The change of the positions of the two substituents on ring 2 would affect its geometrical characteristics, leading to $\theta \approx 54{\cdot}7°$ being between the principal axis and the C6–H6 vector in **6RCl** and **6RCH3** [equation (3)], leaving only the C6–H7 coupling. On the other hand, ring 1 is not directly affected by the substituents, and certainly no change in its geometrical characteristics is expected due to the relative lack of conjugation between rings 1 and 2 through the azo bond as evidenced by the X-ray structure (to be discussed later). These qualitative arguments can be verified by studying the ^{13}C chemical shifts, which are more sensitive with respect to change in temperature.

3.4. *Chemical shift changes of the aromatic rings*

The aromatic part of the chemical shifts of the phenyl carbons in **6RCl** plotted against the reduced temperature is presented in figure 6. The data show that the temperature dependences of various carbons in **6RCl** are quite different. Plots obtained for **6LCl**, **6RCH3** and **6LCH3** are similar. Only carbons belonging to the lateral branch and carbons C6 and C7 present a temperature dependence of the chemical shift which does not overlap with that found for **6RCl**, meaning again that the change of terminal substituent or aromatic branch location does not affect the ordering of the whole molecule.

The ^{13}C chemical shift changes can be related to the macroscopic order parameter by the semi-empirical equation [21]:

$$\delta_{obs} = \delta_{iso} + aS_{zz} + b \qquad (4)$$

where a and b are constants which are assumed to be independent of temperature within experimental error. Usually $a \gg b$, and $a \approx (2/3)\,[\sigma_{zz} - (\sigma_{xx} + \sigma_{yy})/2]$ for the quaternary carbons when the *para*-axis is nearly aligned with the molecular long axis. If we assumed a Haller [22] type dependence of the order parameter versus

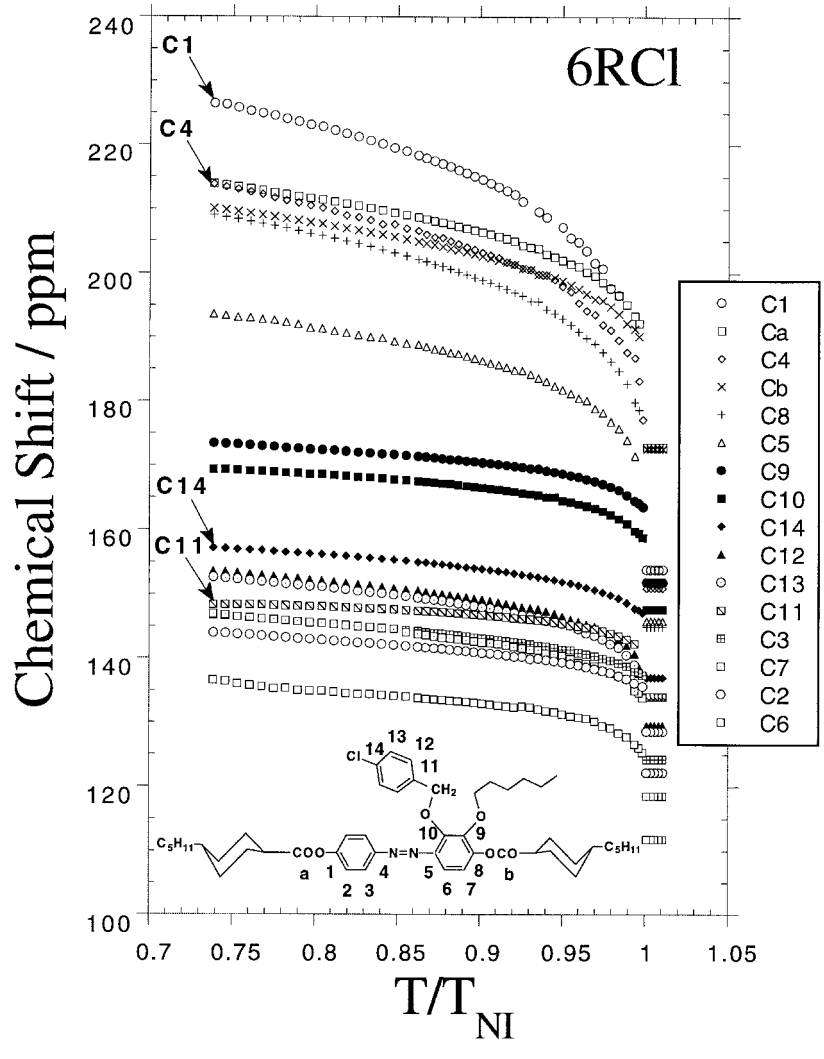

Figure 6. Aromatic part of the chemical shift in **6RCl** obtained with slow spinning of the sample parallel to the magnetic field. Assignment was made by using the F value obtained from equation (4). Some assignments in the same ring may be inverted (C9, C10; C2, C3; C12, C13 for example).

temperature, δ_{obs} is given by:

$$\delta_{obs} = A + B*(1 - T/T^{\dagger})^{F} \quad (5)$$

where $A = \delta_{iso} + b$ and $B = S_o * a$. The carbons belonging to the same *para*-disubstituted ring must have the same S_o and F values. This can be used to help the assignment of different peaks in the spectrum. Then, constant b can be estimated from A using the isotropic chemical shift of each carbon. Thus, all the temperature dependences having a noticeable chemical shift anisotropy were fitted with equation (4) using the four parameters A, B, $T^{\dagger}$ and F. $T^{\dagger}$ was found to be slightly higher than T_{NI} by $0{\cdot}5 \sim 1$ K, depending on the compound. In the second part of the calculation, $T^{\dagger}$ was fixed at an average value for each compound, and each set of data was refitted with only three parameters. The four carbons in each *para*-substituted ring have the similar F values that are summarized in table 4. Usually, a large F value is correlated with a more rigid fragment. The rigidity of a fragment depends on its structure and on its interaction with nearby fragments. Because of the strong steric interaction between the core and the methyleneoxy fragment within the lateral chain (azo link and the aromatic branch), the lateral aromatic branch is the most rigid fragment. This means that its ordering increases slowly with decreasing temperature due to the lack of flexibility of the methyleneoxy fragment. The tetra-substituted ring 2 has a lower symmetry than the *para*-disubstituted ring. As a consequence, the temperature dependence of its carbons is more complex, and the F values obtained for various carbons on the same ring are different and more scattered. In each compound, F values obtained for C9 and C10 are systematically smaller ($0{\cdot}07 \pm 0{\cdot}02$) than the other values ($0{\cdot}11 \pm 0{\cdot}03$). This can be related to the effect of the directly attached substituents on the ordering process of that ring.

The lack of dipolar splittings for the lateral branch has not permitted the evaluation of the ordering of that ring. However, the differential orientation of the lateral branch can be estimated through the chemical shift evolution of these carbons. In conventional mesogens, the quaternary carbons usually have the largest anisotropy due to the particular position of the *para*-axis with respect to the frame of the chemical shift tensor. If we assumed that $S_{zz} \gg S_{xx} - S_{yy}$, the value of $\delta_{obs} - \delta_{iso}$ should be directly proportional to the S_{zz} value. Figure 7 shows the quaternary carbons C11 and C14 have much smaller anisotropy than carbons C1 and C4. This means that S_{zz} for ring 3 is far less than that for ring 1 due to the tilt of the *para*-axis in the lateral branch. Furthermore, the anisotropy for C1 and C4 is independent of the lateral branch, but that of C11 and C14 depends on the position of the lateral branch and the type of the terminal substituent (figure 7): values for the **L** compounds are much larger than those for the **R** compounds. Apparently, the *para*-axis of the lateral branch makes an angle closer to the magic angle with respect to the major axis when the lateral branch points towards the centre of the molecule, as in the **R** compounds. This result is consistent with the 60° angle found by X-ray measurements, which is discussed in the next section. If the lateral aromatic branch points towards the end part of the molecule, the corresponding angle is farther away from the magic angle as indicated by the larger anisotropy, as in the **L** compounds.

Table 4. Mean values of the F exponent for the two *para*-disubstituted aromatic rings in the four compounds studied as determined by fitting the chemical shifts using equation (3). The absolute error in the mean F values is estimated at $\pm 0{\cdot}03$.

Position	Ring 1	Ring 3
6RCH3	0·15	0·30
6LCH3	0·21	0·50
6RCl	0·16	0·35
6LCl	0·17	0·49

3.5. *X-ray analysis*

Two independent molecules (noted A and B) are found in the crystal cell. The Snoopi drawing [23] of both molecules is presented in figures 8(*a*) and 8(*b*) with the atom labelling of non-hydrogen atoms for both molecules. The thermal B_{eq} factors are rather high for the atoms of the octyloxy chains and increase from the beginning to the end of those chains. This gives imprecise values for a few bond lengths, characterized by high standard deviations. The bond lengths are in good agreement with those found in structures of similar compounds for the core and the octyloxy chains, with the exception of the three C–C bond lengths located at their extremities [7, 24].

The five phenyl rings in both A and B molecules—Φ_{1A} (C1 to C6); Φ_{2A} (C10 to C15); Φ_{3A} (C20 to C25); Φ_{4A} (C30 to C35); Φ_{5A} (C50 to C55); Φ_{1B} (C101 to C106); Φ_{2B} (C110 to C115); Φ_{3B} (C120 to C125); Φ_{4B} (C130 to C135); Φ_{5B} (C150 to C155)—are perfectly planar. The values of the torsion angles, which entirely define the geometry of both molecules are given in table 5. The polyaromatic core conformations essentially differ for the two molecules by the torsions around flexible carboxylate linkages. The terminal 4-methylbenzoate and 4-chlorobenzoate groups are more or less planar, but have different tilt angles with respect to the bonded aromatic ring. The central part $\Phi_{1A,B}$–N=N–$\Phi_{2A,B}$, which is assumed to be rigid, is not planar, and

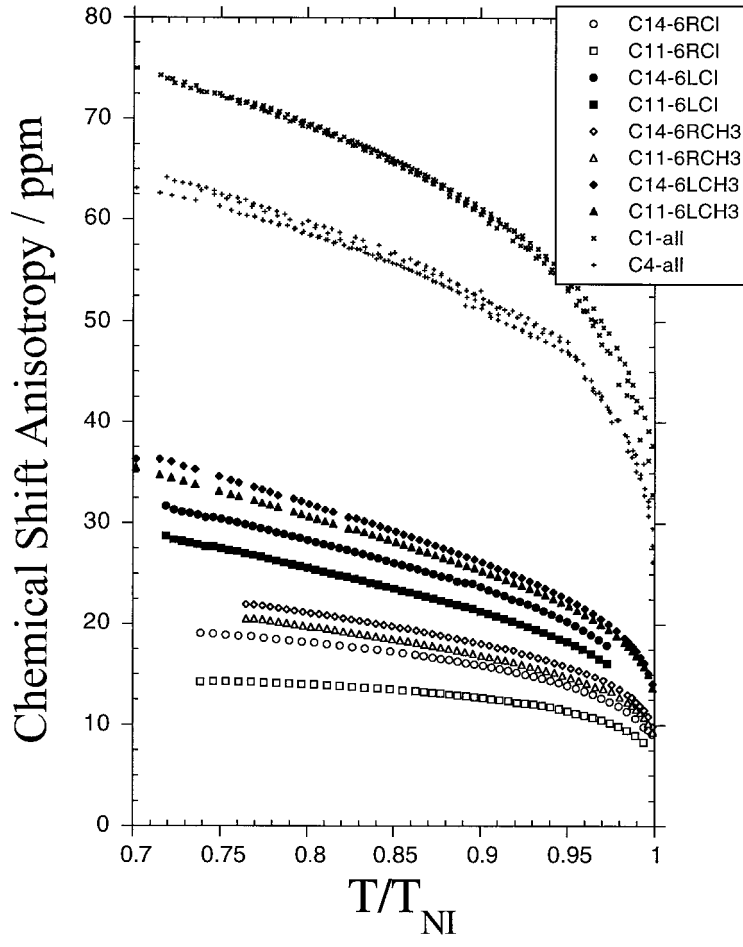

Figure 7. Comparison of the chemical shift anisotropy for C1, C4, C11 and C14 carbons belonging to the aromatic lateral branch in the four compounds **6LCl**, **6RCl**, **6LCH3**, **6RCH3**.

deviations up to 20° are observed. However, the polyaromatic central cores are rather extended as can be seen in the values of the angles:

$$\alpha(\mathrm{C18}\ldots\mathrm{N16}\ldots\mathrm{Cl29}) = 168{\cdot}0(6)^\circ$$

$$\alpha(\mathrm{C118}\ldots\mathrm{N116}\ldots\mathrm{Cl129}) = 165{\cdot}5(5)^\circ.$$

Replacing the benzoate groups by the pentylcyclohexane carboxylate groups would slightly affect the geometry of the central part of the core.

The conformation of the lateral 4-chlorobenzoyl groups and their orientations relative to the polyaromatic cores are similar in both A and B molecules (the torsions around C25–O45 and C125–O145; O45–C46 and O145–C146; C46–C50 and C146–C150 are almost identical). They make an angle close to 60° with the polyaromatic core.

The octyloxy lateral chains in both molecules are folded back along their own central cores. This can be compared to the chain conformations found in some related compounds with two lateral chains [25] or one lateral chain and a nearby methyl group [24]. Due to the steric hindrance between the two substituents on the same side of the ring, the two first fragments, C20–C25–O45–C46 and C23–C24–O36–C37 are nearly in *gauche*-conformations, pointing in opposite directions with respect to the mean aromatic plane. After this first fragment, *trans*-conformations are found with the exception of the far part of the flexible chain. In addition, the two molecules essentially differ by the torsion angles around the C40–C41 and C140–C141, C41–C42 and C141–C142 bonds.

Finally, both A and B molecules have similar conformations with the exception of the terminal octyloxy lateral chains and are characterized by the following dihedral angles:

$$[\Phi_{2A}/\Phi_{1A} = 85{\cdot}0(2)^\circ,\ \Phi_{3A}/\Phi_{2A} = 35{\cdot}5(2)^\circ,$$

$$\Phi_{4A}/\Phi_{3A} = 83{\cdot}6(2)^\circ,\ \Phi_{5A}/\Phi_{3A} = 21{\cdot}6(2)^\circ]$$

$$[\Phi_{2B}/\Phi_{1B} = 63{\cdot}8(2)^\circ,\ \Phi_{3B}/\Phi_{2B} = 41{\cdot}7(2)^\circ,$$

$$\Phi_{4B}/\Phi_{3B} = 70{\cdot}7(2)^\circ,\ \Phi_{5B}/\Phi_{3B} = 27{\cdot}1(2)^\circ].$$

Because of the $P1$ space group, both A and B molecular core axes are almost parallel. Moreover, the dihedral

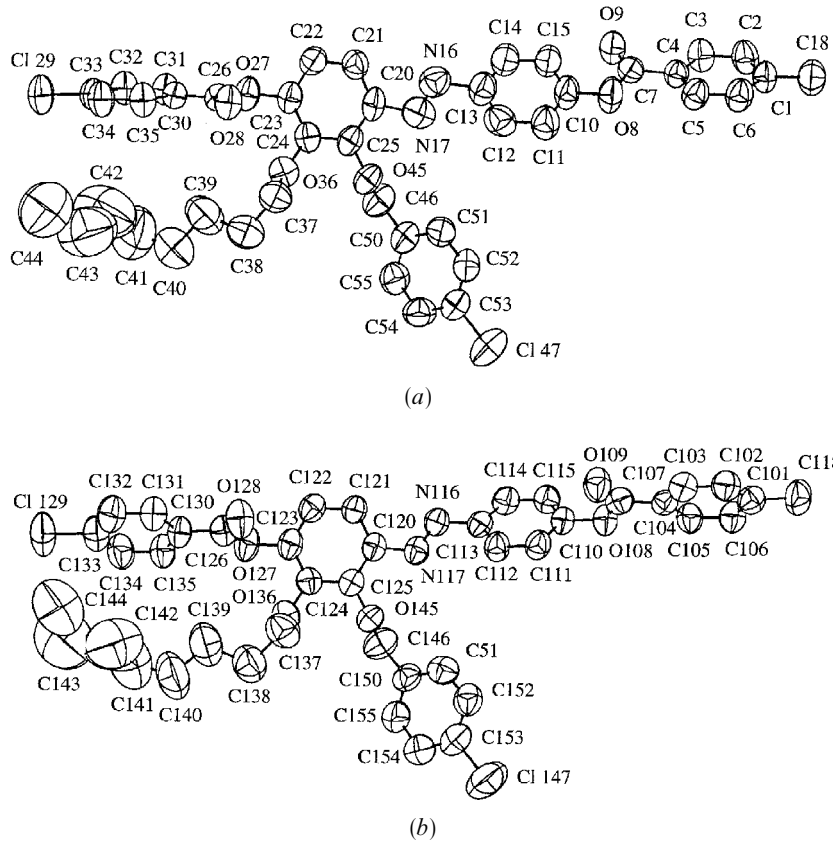

Figure 8. SNOOPI drawing of both (*a*) A and (*b*) B independent molecules including the atom labelling. Displacement ellipsoids are drawn at the 50% probability level.

Table 5. Significant[a] torsion angles (°) with standard deviations in brackets.

Dihedral angle	Value	Dihedral angle	Value
C3–C4–C7–C8	169·2(5)	C103–C104–C107–C108	*trans*
C7–C8–C10–C11	−83·2(5)	C107–C108–C110–C111	113·0(5)
C12–C13–N16–N17	−163·7(6)	C112–C113–N116–N117	164·7(5)
C13–N16–N17–C20	*trans*	C113–N116–N117–C120	*trans*
N16–N17–C20–C25	−168·7(5)	N116–N117–C120–C125	161·7(5)
C22–C23–O27–C26	−98·4(5)	C122–C123–O127–C126	−81·4(5)
C23–O27–C26–C30	*trans*	C123–O127–C126–C130	*trans*
O27–C26–C30–C31	*trans*	O127–C126–C130–C131	*trans*
C20–C25–O45–C46	−99·6(5)	C120–C125–O145–C146	−91·2(5)
C25–O45–C46–C50	168·5(7)	C125–O145–C146–C150	169·6(5)
O45–C46–C50–C51	−57·2(5)	O145–C146–C150–C151	−60·2(5)
C23–C24–O36–C37	−110·1(5)	C123–C124–O136–C137	−106·8(4)
C24–O36–C37–C38	*trans*	C124–O136–C137–C138	167·8(5)
O36–C37–C38–C39	−61·1(6)	O136–C137–C138–C139	−69·7(6)
C37–C38–C39–C40	*trans*	C137–C138–C139–C140	*trans*
C38–C39–C40–C41	*trans*	C138–C139–C140–C141	*trans*
C39–C40–C41–C42	−68(1)	C139–C140–C141–C142	−89(1)
C40–C41–C42–C43	−60(1)	C140–C141–C142–C143	−169(1)
C41–C42–C43–C44	−163(1)	C141–C142–C143–C144	−160(1)

[a] Angles which differ by more than 10° from those in the *trans*-conformation (180°).

angles between homologuous phenyl groups in both molecules are very similar.

$$[\Phi_{1B}/\Phi_{1A} = 13{\cdot}2(2)^\circ,\ \Phi_{2B}/\Phi_{2A} = 8{\cdot}2(2)^\circ,$$

$$\Phi_{3B}/\Phi_{3A} = 3{\cdot}7(2)^\circ,\ \Phi_{4B}/\Phi_{4A} = 14{\cdot}6(2)^\circ].$$

As can be seen on the projection of the crystal structure on the (*xoy*) plane (figure 9), all molecular axes are parallel, giving a molecular arrangement typical of a nematogenic compound. The crystal packing is mostly assumed through several weak van der Waals interations,

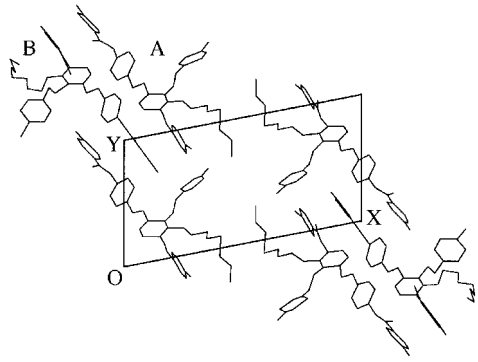

Figure 9. Projection of the crystal structure on the (*xoy*) plane.

in agreement with the relatively low density of the crystal ($1{\cdot}257\,g\,cm^{-3}$).

4. Conclusion

We have synthesized new nematic compounds containing two aromatic and two alicyclic rings in the main core and two lateral substituents on one of the phenyl rings. One of the lateral substituents is a hexyloxy chain and the other a *para*-substituted benzyloxy branch. These compounds deviate markedly from the classical rod shape, but they exhibit a wide nematic range which is only slightly dependent on the relative position and type of the lateral aromatic branch. By applying 1-D and 2-D ^{13}C NMR techniques, the orientational ordering of the aliphatic chains and the aromatic rings has been studied. The two lateral substituents are folded back along the mesogenic core, involving a *gauche*-conformation for the first fragment. The lateral chain is more or less aligned with the molecular long axis. But the *para* axis of the aromatic ring in the lateral branch makes an angle with the core close to the magic angle with that axis. On the contrary, the molecular long axis is not much influenced by the pattern of disubstitution. The X-ray structure of one parent compound indicates that the molecular conformation in the solid phase is not much different from that observed in the nematic phase. Further work is under way and shows that bulkier substituents may be introduced without affecting the liquid crystal properties.

The work of B.M.F. was supported by the US National Science Foundation under grant number DMR-9321114 and DMR-9700680.

References

[1] Perez, F., Judeinstein, P., Bayle, J.-P., Roussel, F., and Fung, B. M., 1997, *Liq. Cryst.*, **22,** 711.
[2] Demus, D., 1989, *Liq. Cryst.*, **5,** 75.
[3] Attard, G. S., and Imrie, C. T., 1989, *Liq. Cryst.*, **6,** 387.
[4] Nguyen, H. T., and Destrade, C., 1989, *Mol. Cryst. liq. Cryst. Lett.*, **6,** 123.
[5] Ballauf, M., 1987, *Liq. Cryst.*, **2,** 519.
[6] Imrie, C. T., and Taylor, L., 1989, *Liq. Cryst.*, **6,** 1.
[7] Perez, F., Berdagué, P., Judeinstein, P., Bayle, J.-P., Allouchi, H., Chasseau, D., Cotrait, M., and Lafontaine, E., 1995, *Liq. Cryst.*, **19,** 1015.
[8] Perez, F., Bayle, J.-P., and Fung, B. M., 1996, *New J. Chem.*, **20,** 537.
[9] Berdagué, P., Perez, F., Bayle, J.-P., Ho, M. S., and Fung, B. M., 1995, *New J. Chem.*, **19,** 383.
[10] Berdagué, P., Perez, F., Courtieu, J., and Bayle, J.-P., 1993, *Bull. Soc. Chim. Fr.*, **130,** 475.
[11] Hassner, A., and Alexanian, V., 1978, *Tetrahedron Lett.*, **46,** 4475.
[12] Nose, A., and Kudo, T., 1981, *Chem. Phar. Bull.*, **29,** 1159.
[13] Franz, B. A. & Associates Inc., 1982, *SDP Structure Determination Package*, College Station, Texas, USA.
[14] Sheldrick, G. M., 1985, *SHELXS86*, Program for the Solution of Crystal Structures, Univ. of Götingen, Germany.
[15] Fung, B. M., 1996, in *Encyclopedia of Nuclear Magnetic Resonance*, edited by D. M. Grant and R. K. Harris (Wiley), p. 2744.
[16] Bayle, J.-P., Ho, M. S., and Fung, B. M., 1993, *New J. Chem.*, **17,** 345.
[17] Osman, M. A., 1985, *Mol. Cryst. liq. Cryst.*, **128,** 45.
[18] Perez, F., Judeinstein, P., and Bayle, J. P., 1995, *New J. Chem.*, **19,** 1015.
[19] Perez, F., Judeinstein, P., Bayle, J.-P., Brauniger, T., and Fung, B. M., 1996, *New J. Chem.*, **20,** 1175.
[20] Magnuson, M. L., Fung, B. M., and Bayle, J.-P., 1995, *Liq. Cryst.*, **19,** 823.
[21] Guo, W., and Fung, B. M., 1991, *J. chem. Phys.*, **95,** 3917.
[22] Haller, I., 1975, *Prog. Solid State Chem.*, **10,** 103.
[23] Davies, K., 1983, *SNOOPI*, Program for Drawing Crystal and Molecular Diagrams Chemical Laboratory, University of Oxford, England.
[24] Perez, F., Berdague, P., Judeinstein, P., Bayle, J.-P., Allouchi, H., Cotrait, M., and Lafontaine, E., 1996, *Liq. Cryst.*, **21,** 855.
[25] Perez, F., Berdagué, P., Judeinstein, P., Bayle, J.-P., Allouchi, H., Cotrait, M., and Lafontaine, E. (to be published).